

Recent results on the mathematical modelling of the cardiovascular system

L. Formaggia

MOX - Modelling and Scientific Computing, Politecnico di Milano



Numerical analysis day, 18th September 2006, Bologna

Summary of the talk

Part1: motivations and examples

- Why to simulate blood flow?
- Altered flow conditions
- Surgical planning
- Prosthesis design

Part2: coupling 3D and 1D models of the cardiovascular system

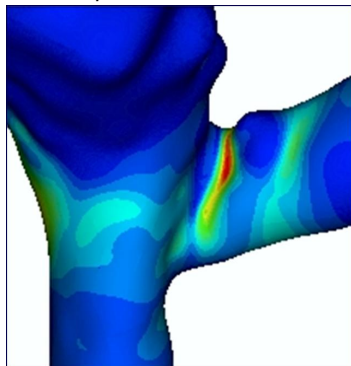
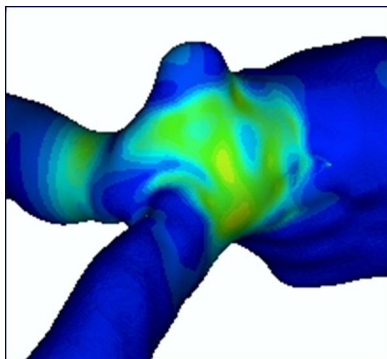
- The 3D FSI model
- The 1D FSI model
- Coupling 3D and 1D models
- The discrete problem
- Some numerical results
- Conclusions

Why to simulate blood flow?

- ▶ A number of vascular diseases are linked to local haemodynamics. For instance *atherosclerosis* and *cerebral aneurisms* → **medical research**
- ▶ Altered flow conditions following a surgical operation like a *by-pass* may have negative effect and cause post-surgical failures → **surgical planning**
- ▶ The design of a prosthesis or other devices (like a stent) may be aided by haemodynamic simulations → **prosthesis design**
- ▶ A simulator of the cardiovascular system may well serve for training medical doctor and anesthesiologists → **training**

Altered fluid-dynamics due to stenoses

Wall shear stress map



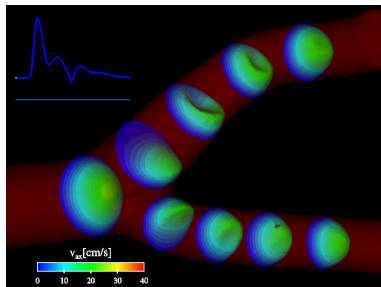
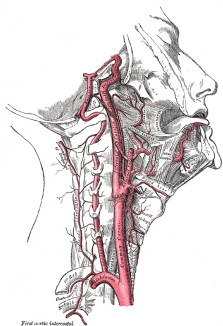
Wall shear stress (WSS) in a stenosed area may reach the value of 25–30 dyne/cm² compared to the physiological values of around 4–6 dyne/cm²

$$\mathbf{WSS} = \boldsymbol{\sigma}(\mathbf{u}, p)\mathbf{n} - (\mathbf{n}^T \boldsymbol{\sigma}(\mathbf{u}, p)\mathbf{n})\mathbf{n}$$

$\boldsymbol{\sigma}(\mathbf{u}, p)$ is the *Cauchy stress tensor*

$$\boldsymbol{\sigma}(\mathbf{u}, p) = \mu(\nabla\mathbf{u} + \nabla^T\mathbf{u}) - p\mathbf{I}$$

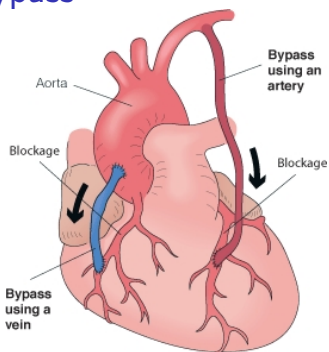
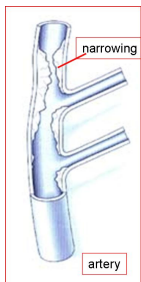
Blood recirculation regions



Computation by M. Prosi

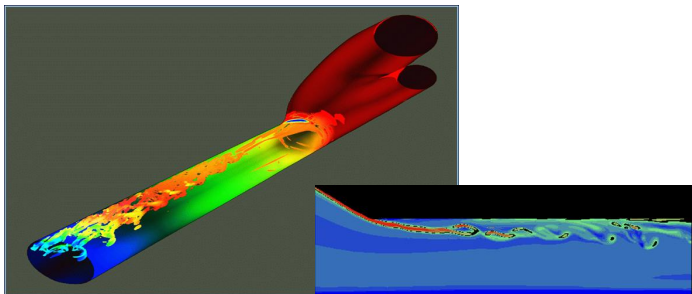
Recirculation region in areas like the *carotid sinus* may cause oscillation of the wall shear stresses \rightarrow damage to the endothelium \rightarrow inflammatory process \rightarrow arteriosclerosis

Vortex generation around a bypass



A by-pass is created to bring blood to a part of the myocardium that has been partially or totally excluded because of a stenosis (narrowing of the lumen) in a coronary artery

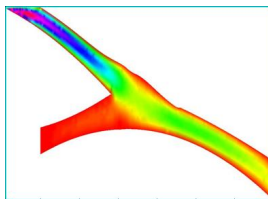
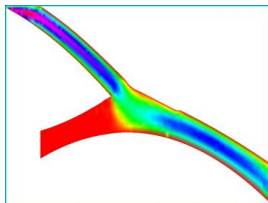
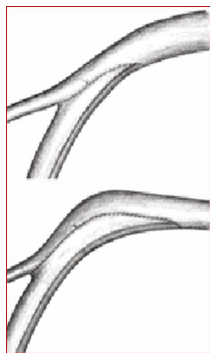
Vortex generation around a bypass



The flow around a bypass is altered and may initiate inflammatory processes which may lead to a stenosis. We need to reduce the generation of vorticity.

F. Loth, S. Lee and F. Fisher

Optimization of the shape of a by-pass

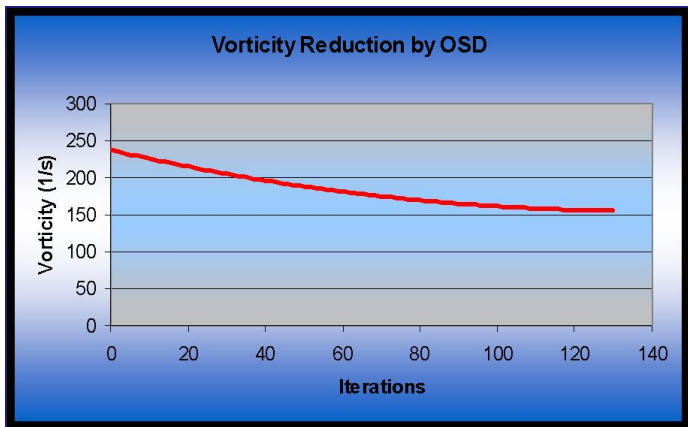


On the right the result by an automatic optimisation procedure which reduced the average vorticity by 45%. On the left the *Miller* cuff, a surgical procedure adopted for a by-pass.

G. Rozza, V. Agoskov, A. Quarteroni

Problem: find the shape so that $\|\text{curl } \mathbf{u}\|_{L^2(\Omega)}$ is minimized.

Optimization procedure results



Design of an endograft for AAA

Abdominal aortic aneurysms (AAA) is a significant and important vascular disease. They are characterised by an abnormal dilatation of a portion of the aorta. This swollen region would enlarge with time and, without a surgical treatment, it will eventually break with fatal consequences.

Design of an endograft for AAA

Abdominal aortic aneurysms (AAA) is a significant and important vascular disease. They are characterised by an abnormal dilatation of a portion of the aorta. This swollen region would enlarge with time and, without a surgical treatment, it will eventually break with fatal consequences.

Exclusion of abdominal aortic aneurysms



abdominal aortic aneurysm



replacement of the aorta



endoluminal exclusion of abdominal aortic aneurysm

Design of an endograft for AAA

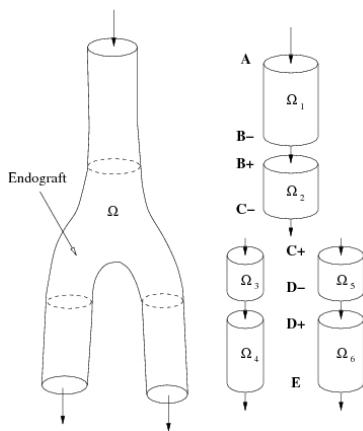
Abdominal aortic aneurysms (AAA) is a significant and important vascular disease. They are characterised by an abnormal dilatation of a portion of the aorta. This swollen region would enlarge with time and, without a surgical treatment, it will eventually break with fatal consequences.

An endograft



Design of an endograft for AAA

Abdominal aortic aneurysms (AAA) is a significant and important vascular disease. They are characterised by an abnormal dilatation of a portion of the aorta. This swollen region would enlarge with time and, without a surgical treatment, it will eventually break with fatal consequences.



Note: The change of mechanical characteristics has been handled by a **domain decomposition approach** and imposing continuity of fluxes and total pressure at the interface (L.F. D.Lamponi A. Quarteroni).

Numerical Simulation

$\rho = 1 \text{ gr/cm}^3$, $\nu = 0.035 \text{ cm}^2/\text{s}$, $\alpha = 1$, $h_0 = 0.05 \text{ cm}$; $E_{\text{endograft}} = 60 \cdot 10^6 \text{ dyne/cm}^2$ for the endografted part (Ω_i , $i = 2, 3, 5$) and $E_{\text{vessel}} = 10 \cdot 10^6 \text{ dyne/cm}^2$ for the remaining subdomains. The vessel reference radii are $R_{0,1} = R_{0,2} = 0.6 \text{ cm}$, $R_{0,3} = R_{0,4} = 0.4 \text{ cm}$ and $R_{0,5} = R_{0,6} = 0.5 \text{ cm}$.

At inlet we have imposed a half sine pressure wave of period 0.1 s and amplitude 20000 dyne/cm^2 .

The spatial grid was of 546 nodes and $\Delta t = 1 \times 10^{-4} \text{ s}$.

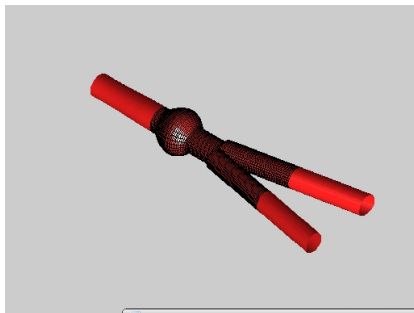
Numerical Simulation

ANIMATIONS

Stiffer

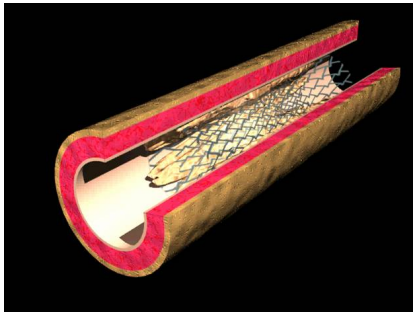
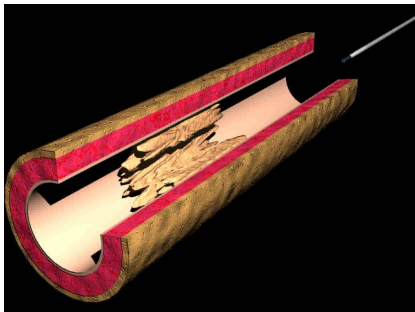


Softer

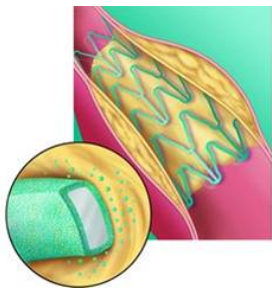


Design of stents

Stents are expandable metallic wires used to cure stenosis caused by lipid plaques. They are expanded by means of a balloon and implanted in the vessel wall



Drug eluting stents



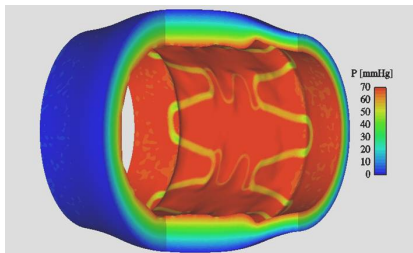
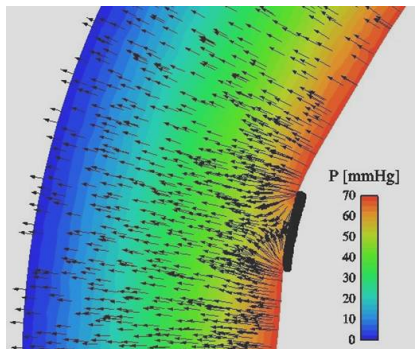
A new generation of stents is covered by a layer of a polymeric substance filled with anti-inflammatory drug. The aim is to reduce the risk of inflammation of the vessel tissue after implant

$$\frac{\partial c_w}{\partial t} + \frac{\gamma_w}{k_w} (\mathbf{u}_w \cdot \nabla) c_w - D_w \Delta c_w = 0$$

$$\mathbf{u}_w = -\frac{K_p}{\mu_p} \nabla p, \quad \nabla \cdot \mathbf{u}_w = 0$$

Special interface conditions to simulate the drug dissolution in the polymeric matrix.

Simulation of the elution process



P. Zunino, M. Prosi, F. Gervaso, S. Minisini

Part2: coupling 3D and 1D models of the cardiovascular system

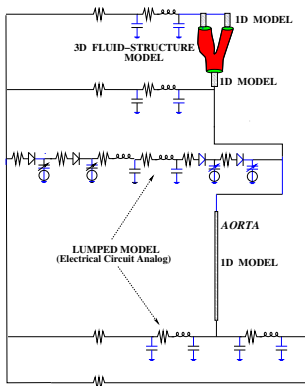
The complexity of the haemodynamic problem

► In the arterial tree:

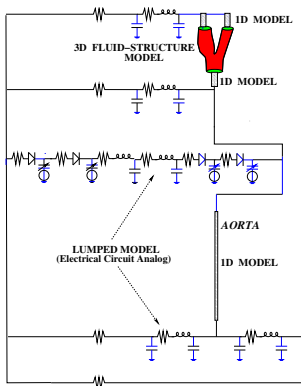
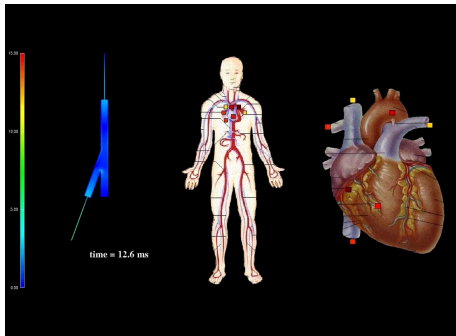
pulsatile flow	⇒	unsteady problem
very complex and heterogeneous geometry	⇒	fully 3D simulations restricted to specific regions of interest
global circulation influences local flow dynamics	⇒	need to account for the remaining parts
pulse propagation	⇒	need for fluid-structure interaction algorithms and appropriate absorbing boundary conditions

Motivation: the need of different models

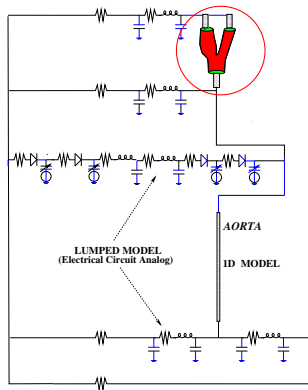
- ▶ Simulations of large parts of the arterial tree require using different models, with different spatial dimensions and level of accuracy, and to couple them together
- ▶ The mutual influence between the local problem and the global circulation requires to account for the local/global interplay



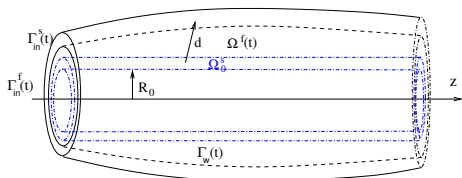
Motivation: the need of different models



Motivation: the need of different models

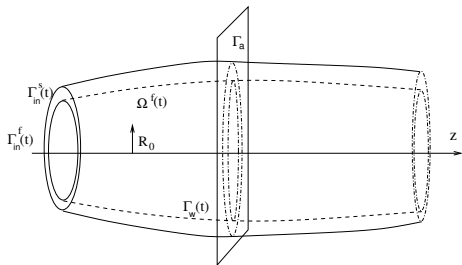


The model reduction procedure



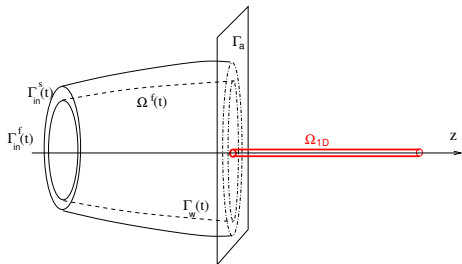
Fluid-structure interaction problem in a cylindrical-type geometry representing an artery

The model reduction procedure



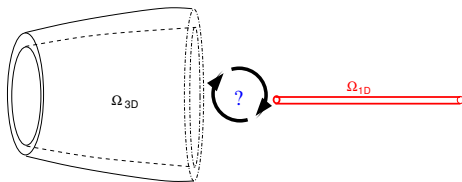
Decompose the geometry into two parts: one will be represented by a reduced one-dimensional model

The model reduction procedure



Devise an appropriate reduced model

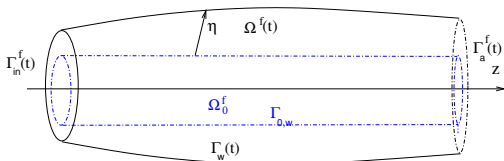
The model reduction procedure



Find appropriate coupling condition and numerical strategies

The 3D model: fluid equations

Navier-Stokes, curl formulation, ALE frame



$$\mathcal{A}_t : \Omega_0^f \rightarrow \Omega^f(t)$$

$$\mathbf{w} = \frac{\partial \mathcal{A}_t}{\partial t}$$

$$P = p + \frac{\rho}{2} |\mathbf{u}|^2$$

$$\mathbf{D}(\mathbf{u}) = \frac{1}{2} (\nabla \mathbf{u} + \nabla^T \mathbf{u})$$

$$\begin{aligned} \Delta \mathcal{A}_t &= 0, & \text{in } \Omega_0^f \\ \mathcal{A}_t &= 0 & \text{on } \partial \Omega_0^f \setminus \Gamma_{0,w} \\ \Omega^f(f) &= \mathcal{A}_t(\Omega_0^f) \end{aligned}$$

$$\rho \frac{\partial \mathbf{u}}{\partial t} \Big|_{\mathcal{A}} + \rho \operatorname{curl} \mathbf{u} \times \mathbf{u} - \rho (\mathbf{w} \nabla) \mathbf{u} + \nabla P - \operatorname{div}(2\mu \mathbf{D}(\mathbf{u})) = \mathbf{0} \quad \text{in } \Omega^f(t)$$

$$\operatorname{div} \mathbf{u} = 0 \quad \text{in } \Omega^f(t)$$

$$\mathbf{u} = \mathbf{u}_{in} \quad \text{on } \Gamma_{in}^f(t)$$

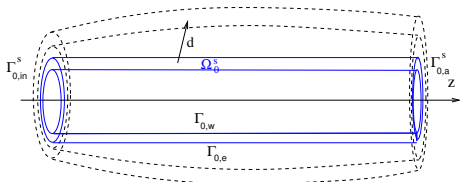
$$P - (2\mu \mathbf{D}(\mathbf{u}) \cdot \mathbf{n}^f) \cdot \mathbf{n}^f = q, \quad \mathbf{u} \times \mathbf{n}^f = \mathbf{0} \quad \text{on } \Gamma_a^f(t)$$

for all $t \in (0, T)$ and with appropriate initial conditions.

Note: no conditions on FS interface have been provided yet.

The 3D model: structure equations

Elastic material in large displacement, Lagrangian formulation



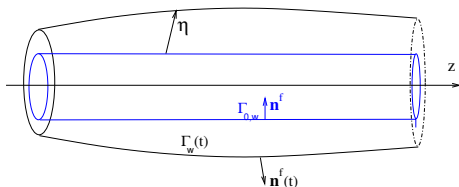
$$\begin{aligned}\boldsymbol{\sigma}^s(\mathbf{d}) &= (\mathbf{I} + \nabla \mathbf{d}) \mathbf{S}(\mathbf{d}) \\ \mathbf{S}(\mathbf{d}) &= \lambda \operatorname{tr}(\mathbf{E}) \mathbf{I} + 2\mu^s \mathbf{E} \\ \mathbf{E} &= \frac{1}{2} (\nabla \mathbf{d} + \nabla^T \mathbf{d} + \nabla^T \mathbf{d} \nabla \mathbf{d})\end{aligned}$$

$$\begin{aligned}\rho_s \frac{\partial^2 \mathbf{d}}{\partial t^2} - \operatorname{div} \boldsymbol{\sigma}^s(\mathbf{d}) &= \mathbf{0} \quad \text{in } \Omega_0^s \\ \boldsymbol{\sigma}^s(\mathbf{d}) \cdot \mathbf{n}^s &= p_e \mathbf{n}^s \quad \text{on } \Gamma_{0,e} \\ \mathbf{d} &= \mathbf{g} \quad \text{on } \Gamma_{0,in} \\ (\boldsymbol{\sigma}^s(\mathbf{d}) \cdot \mathbf{n}^s) \times \mathbf{n}^s &= \mathbf{0}, \quad \mathbf{d} \cdot \mathbf{n}^s = 0 \quad \text{on } \Gamma_{0,a,e}^s\end{aligned}$$

for all $t \in (0, T)$ and with appropriate initial conditions for \mathbf{d} and $\partial_t \mathbf{d}$.

Note: no conditions on FS interface have been provided yet.

The 3D model: fluid-structure interface conditions



On $\Gamma_{0,w}$ we set $\boldsymbol{\eta} = \mathbf{d}$ and

$$\begin{aligned} \mathcal{A}_t &= \boldsymbol{\eta} \\ \mathbf{u} \circ \mathcal{A}_t &= \frac{\partial \boldsymbol{\eta}}{\partial t} \\ (\boldsymbol{\sigma}^f(\mathbf{u}, p) \cdot \mathbf{n}^f(t)) \circ \mathcal{A}_t + \boldsymbol{\sigma}^s(\mathbf{d}) \cdot \mathbf{n}^s &= \mathbf{0} \end{aligned}$$

where $\boldsymbol{\sigma}^f(\mathbf{u}, p) = -p\mathbf{l} + 2\mu\mathbf{D}(\mathbf{u})$.

These conditions express continuity of velocity and stresses at the interface.

The 3D model: known result

- **Energy estimate**

$$\mathcal{E}_{3D} = \frac{\rho}{2} \|\mathbf{u}\|_{L^2(\Omega^f(t))}^2 + \frac{\rho^s}{2} \|\partial_t \mathbf{d}\|_{L^2(\Omega_0^s)}^2 + \mu^s \|\mathbf{E}\|_{L^2(\Omega_0^s)}^2 + \frac{\lambda}{2} \|\operatorname{tr}(\mathbf{E})\|_{L^2(\Omega_0^s)}^2$$

$$\frac{d}{dt} \mathcal{E}_{3D}(t) + C_1 \|\mathbf{u}(t)\|_{H^1(\Omega^f(t))}^2 \leq C_2 \left[|\mathbf{q}(t)|^2 + \|\mathbf{u}_{in}(t)\|_{H^{1/2}(\Gamma_{in}^f(t))}^2 + \|\mathbf{g}(t)\|_{H^{1/2}(\Gamma_{0,in}^s)}^2 \right]$$

- **Well posedness (only partial results, even in the 2D case, often a *viscoelastic term* is added to regularize $\boldsymbol{\eta}$):** Y. Maday, C. Grandmont, B. Desjardins, M. J. Esteban, C. Conca, H. Beirao da Veiga....
- **Development and analysis of numerical methods:** P. Le Tallec, F. Nobile, M.A. Fernández, M. Moubachir, J-F. Gerbeau, S. Deparis, H.G. Matthies, W.A. Wall, ...

The 3D model: known result

- **Energy estimate**

$$\mathcal{E}_{3D} = \frac{\rho}{2} \|\mathbf{u}\|_{L^2(\Omega^f(t))}^2 + \frac{\rho^s}{2} \|\partial_t \mathbf{d}\|_{L^2(\Omega_0^s)}^2 + \mu^s \|\mathbf{E}\|_{L^2(\Omega_0^s)}^2 + \frac{\lambda}{2} \|\operatorname{tr}(\mathbf{E})\|_{L^2(\Omega_0^s)}^2$$

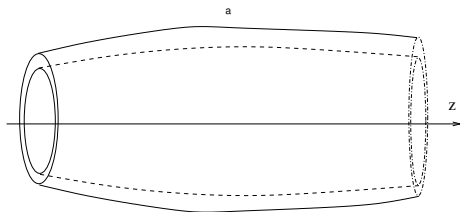
$$\frac{d}{dt} \mathcal{E}_{3D}(t) + C_1 \|\mathbf{u}(t)\|_{H^1(\Omega^f(t))}^2 \leq C_2 \left[|\mathbf{q}(t)|^2 + \|\mathbf{u}_{in}(t)\|_{H^{1/2}(\Gamma_{in}^f(t))}^2 + \|\mathbf{g}(t)\|_{H^{1/2}(\Gamma_{0,in}^s)}^2 \right]$$

- **Well posedness (only partial results, even in the 2D case, often a *viscoelastic term* is added to regularize $\boldsymbol{\eta}$):** Y. Maday, C. Grandmont, B. Desjardins, M. J. Esteban, C. Conca, H. Beirao da Veiga....

- **Development and analysis of numerical methods:** P. Le Tallec, F. Nobile, M.A. Fernández, M. Moubachir, J-F. Gerbeau, S. Deparis, H.G. Matthies, W.A. Wall, ...
Other “shell-type” structural models have been used for this problem. The considerations here made extend to many of them

The 1D model: derivation

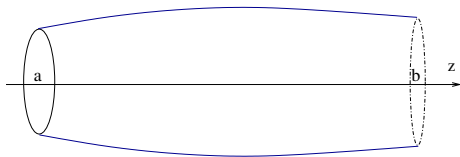
Derived from the 3D-FSI model by



The 1D model: derivation

Derived from the 3D-FSI model by

- ▶ Making some simplifying assumptions:
 - ▶ Cylindrical geometry
 - ▶ Simplified structural models (“shell type” model, linear elastic behaviour)
 - ▶ Neglect wall inertia



The 1D model: derivation

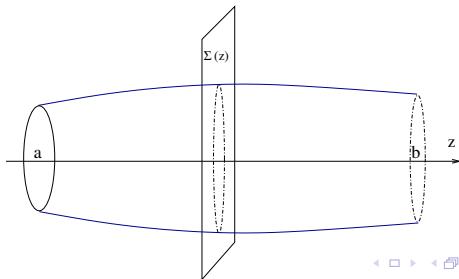
Derived from the 3D-FSI model by

- ▶ Making some simplifying assumptions:
 - ▶ Cylindrical geometry
 - ▶ Simplified structural models (“shell type” model, linear elastic behaviour)
 - ▶ Neglect wall inertia
- ▶ Integrating over the cross section

$$A(z, t) = \int_{\Omega^f(t) \cap \Sigma(z)} d\gamma$$

$$Q(z, t) = \int_{\Omega^f(t) \cap \Sigma(z)} u_z(\mathbf{x}, t) d\gamma$$

$$\bar{p}(z, t) = \int_{\Omega^f(t) \cap \Sigma(z)} p(\mathbf{x}, t) d\gamma$$



The 1D model: derivation

Derived from the 3D-FSI model by

- ▶ Making some simplifying assumptions:
 - ▶ Cylindrical geometry
 - ▶ Simplified structural models (“shell type” model, linear elastic behaviour)
 - ▶ Neglect wall inertia
- ▶ Integrating over the cross section

$$\begin{aligned}
 A(z, t) &= \int_{\Omega^f(t) \cap \Sigma(z)} d\gamma \\
 Q(z, t) &= \int_{\Omega^f(t) \cap \Sigma(z)} u_z(\mathbf{x}, t) d\gamma \\
 \bar{p}(z, t) &= \int_{\Omega^f(t) \cap \Sigma(z)} p(\mathbf{x}, t) d\gamma
 \end{aligned}$$



The 1D model: the equations



It is described by an **hyperbolic system of equations**, endowed with a pressure-area algebraic relation:

$$\left\{ \begin{array}{l} \frac{\partial A}{\partial t} + \frac{\partial Q}{\partial z} = 0, \quad z \in (a, b), t > 0 \\ \frac{\partial Q}{\partial t} + \frac{\partial}{\partial z} \left(\frac{Q^2}{A} \right) + \frac{A}{\rho} \frac{\partial \bar{p}}{\partial z} = -K_r \frac{Q}{A}, \quad z \in (a, b), t > 0 \end{array} \right.$$

$$\bar{p}(A; A_0, \beta) = \beta \frac{\sqrt{A} - \sqrt{A_0}}{A_0} \quad \text{with} \quad \beta = \frac{\sqrt{\pi} h_0 E}{1 - \nu^2}$$

References: T. Pedley, A. Quarteroni and L.F., L.F. and A. Veneziani, S. Canic...

The 1D model: known results

- ▶ It is a full hyperbolic system with characteristic speeds $\lambda_{1,2} = \bar{u} \mp c$, with $\bar{u} = Q/A$ and $c^2 = \frac{A}{\rho} \frac{\partial \bar{p}}{\partial A}$
- ▶ It admits the characteristic variables $W_{1,2} = \bar{u} \pm \int_{A_0}^A \frac{c(s)}{s} ds$
- ▶ Under conditions on the regularity and size of the boundary and initial data it admits global smooth solutions, as well as periodic smooth solution (S. Canic and D. Mirkovic, L.F. D. Amandori S. Ferrari (*submitted*))

Note: In haemodynamic applications $c \ll \bar{u}$ (c of the order of 1 – 10 m/s, \bar{u} of the order of $10^{-3} - 10^{-2}$ m/s).

The 1D Model: boundary conditions

In this work we consider the following boundary conditions for the 1D problem

$$\begin{aligned} \bar{p}(t) + \frac{\rho}{2}\bar{u}^2(t) &= P_{1D}(t), \quad \text{at } z = a \\ W_2(t) &= g_2(t) \quad \text{at } z = b \text{ (non reflecting condition)}. \end{aligned}$$

Let

$$\mathcal{E}_{1D} = \frac{\rho}{2} \int_a^b A \bar{u}^2 dz + \int_a^b \psi(A(z)) dz$$

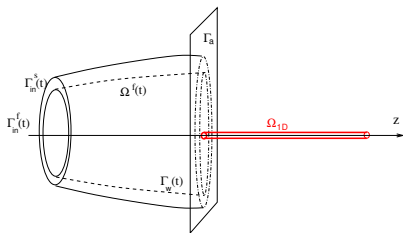
with $\psi(A) = \int_{A_0}^A \bar{p}(s) ds$.

If the initial data are regular enough and such that $c < \bar{u}$ everywhere, g_2 is sufficiently regular and small, then there exists a positive bounded function $G_2 : \mathbb{R} \rightarrow \mathbb{R}^+$ such that, for all $t > 0$

$$\frac{d}{dt} \mathcal{E}_{1D}(t) + Q(a, t) P_{1D}(t) \leq G(g_2(t))$$

This results will allow us to get a **stable** coupling condition.

Coupling 3D and 1D models



At the interface between the 1D and the 3D model we impose

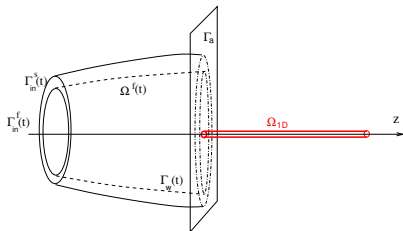
- ▶ Continuity of the flux

$$\int_{\Gamma_a} \mathbf{u} \cdot \mathbf{n} d\gamma = Q(a)$$

- ▶ Continuity of total stress

$$\frac{1}{|\Gamma_a|} \int_{\Gamma_a} p + \frac{\rho}{2} \|\mathbf{u}\|^2 - 2\mu(D(\mathbf{u} \cdot \mathbf{n}) \cdot \mathbf{n}) d\gamma = \bar{p}(a) + \frac{\rho}{2} \bar{u}(a)^2$$

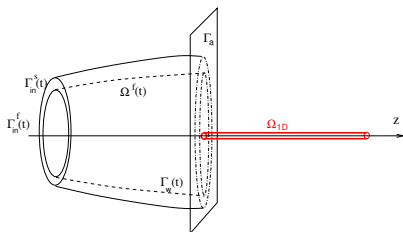
Coupling 3D and 1D models



In fact the condition on the stresses is here imposed to the 3D problem in the form

$$p + \frac{\rho}{2} \|\mathbf{u}\|^2 - 2\mu(D(\mathbf{u} \cdot \mathbf{n}) \cdot \mathbf{n}) = \bar{p}(a) + \frac{\rho}{2} \bar{u}(a)^2, \quad \text{on } \Gamma_a$$

Coupling 3D and 1D models



With this choice of coupling conditions, it is possible to formally derive that for any $T > 0$ the coupled system satisfies

$$[\mathcal{E}_{3D} + \mathcal{E}_{1D}](T) + C_1 \int_0^T \|\mathbf{u}\|_{H^1(\Omega^f)} \leq [\mathcal{E}_{3D} + \mathcal{E}_{1D}](0) + \int_0^T F(\mathbf{u}_{in}(t), \mathbf{g}(t), g_2(t)) dt$$

F being a positive and bounded function of its arguments.

The numerical scheme for each model

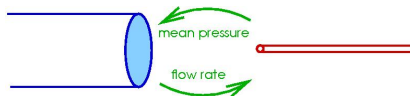
Discretisation of the 1D problem

- ▶ Taylor-Galerkin second-order finite element scheme (linear elements)
- ▶ The solver accounts also for non constant A_0 and variable elastic parameters

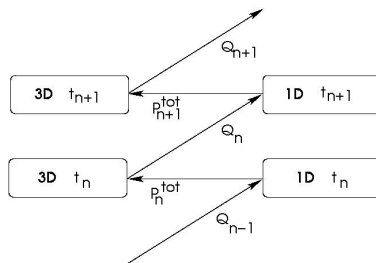
Discretisation of the 3D problem

- ▶ Fluid-structure coupled problem solved implicitly through a Newton iterative algorithm (*M.A. Fernández and M. Moubachir, Computers & Structures, 2005*)
- ▶ Conforming finite element space discretisation for the fluid and structure problems
- ▶ Time discretisation of the structure by a Newmark scheme.

Solving the 3D-1D coupling

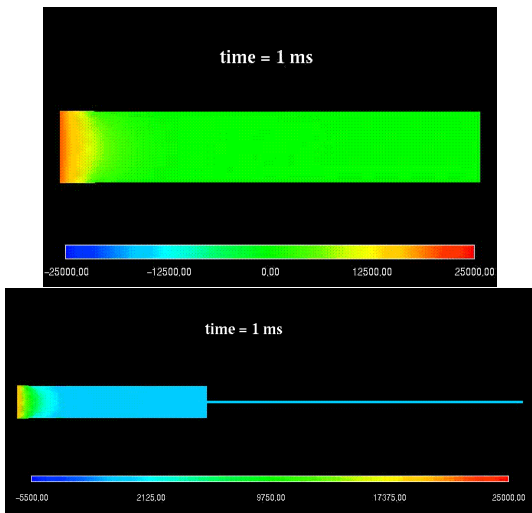


- ▶ The 3D and 1D - are considered separately and solved in a staggered fashion (explicit interface conditions)

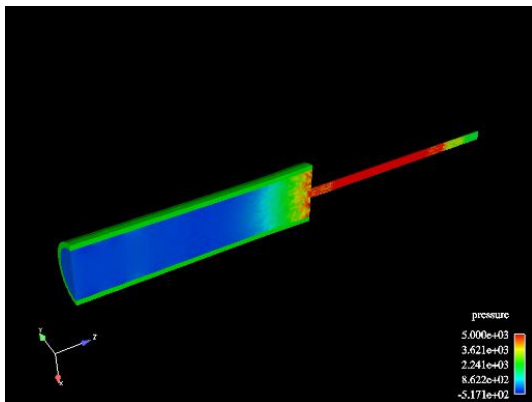


Note: Stability of the staggered scheme under investigation.

An early result

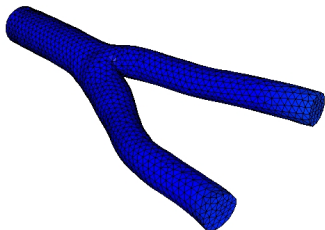


A single artery



A realistic bifurcation

1D models not shown



Conclusions

- ▶ We have devised a stable coupling (at continuous level) between 1D and FSI multidimensional models of blood flow
- ▶ Other coupling conditions are possible like passing the average total stress or the average flux to the 3D model (L.F. A. Veneziani and C. Vergara, L.F. A. Moura, F. Nobile, in preparation). They have not been presented here for the sake of time.
- ▶ Work is ongoing to analyze the full discrete problem. The results of the numerical tests are encouraging.
- ▶ The coupling is now being used for concrete applications such the simulation of blood flow in cerebral aneurysms, using a network 1D description of the main cerebral arteries.

A final remark

The simulation of the circulatory system by means of numerical technique is a very complex and many problems are still open.

Many important aspects have not been covered in this talk:

- ▶ Geometry reconstruction from medical images
- ▶ Simulation of the electrical and mechanical activity of the heart and its interaction with the global circulation
- ▶ Tissue modelling and long term modification
- ▶ Metabolic regulation mechanisms
- ▶ The coagulation process and trombus formation
- ▶ Rheology of blood in small vessels and capillaries
- ▶ ...

Acknowledgments

Most of the simulations were developed in C++ in the scope of the finite element library LifeV (www.lifev.org).

This work has been supported by the European project HaeMOdel (mox.polimi.it/haemodel) , under contract HPRN-CT-2002-002670.

The partial support by the Italian MURST under the project COFIN 2005 and by INDAM is also gratefully acknowledged.

*References and preprints concerning the modeling of the cardiovascular system and related subjects may be found on the **HaeMOdel** site indicated above, at mox.polimi.it and at iacs.epfl.ch/cmcs/publications.php3*